THE DYNAMICS OF THE N-SOLITON, BREATHER, SOLITON MOLECULE, LUMP, AND SEMI-RATIONAL SOLUTION TO NEW $(3+1)$-DIMENSIONAL COMBINED pKP-BKP EQUATION

SIJIE MAO, MAOHUA LI*

School of Mathematics and Statistics, Ningbo University,
Ningbo, Zhejiang 315211, P. R. China
Corresponding author*: limaohua@nbu.edu.cn

Received May 22, 2025

Abstract. The $(3+1)$-dimensional combined pKP-BKP equation is comprehensively explored in this paper. First, N-solitons, breathers, and diverse mixed solutions made up of breathers and kink solitons are among the exact solutions of the $(3+1)$-dimensional combined pKP-BKP equation by using the Hirota bilinear method. Second, lump solutions are obtained from the long-wave limit of the N-solitons and soliton molecules are created through introducing new resonance conditions to the N-solitons. Subsequently, by offering a variety of semi-rational solutions, including lump solutions, kink solitons, and breathers, we enhance the analysis of the $(3+1)$-dimensional combined pKP-BKP equation. The dynamic behavior of these exact solutions is shown using density plots with contour lines and three-dimensional graphs.

Key words: $(3+1)$-dimensional combined pKP-BKP equation, Hirota bilinear method, soliton molecules, lump solutions.

DOI: https://doi.org/10.59277/RomJPhys.2025.70.114

1. INTRODUCTION

The nonlinear evolution equations (NLEEs) serve as fundamental mathematical techniques for characterizing the spatiotemporal development of nonlinear phenomena and they have been used extensively in biology, engineering sciences, physics, and other pertinent domains. The key feature of these equations is the strong influence of nonlinear components on solution behavior, which results in complicated dynamical phenomena including chaos, shock waves, and solitons in physical systems. By using a mathematical model that strikes a balance between nonlinear effects and dispersion effects, these equations highlight underlying regulatory mechanisms controlling complicated wave processes in nature, such as energy transfer in oceanic waves and reliable transmission of optical pulses in fibers. At the application level, the solutions of NLEEs offer theoretical underpinnings for engineering problems ranging from communication system optical signal optimization to fluid dynamics turbulence prediction. Significantly, in-depth studies of these equations in $(3+1)$-dimensional variable-coefficient systems have effectively clarified adaptive waveform propagation mechanisms in non-uniform media. Meanwhile, regarding NLEEs, many

complicated and nonlinear wave phenomena can be characterized by soliton solutions. Therefore, the search for analytic solutions, especially N-soliton solutions, is now becoming increasingly significant in soliton theory. Solitons are natural models that can be used to explain physical phenomena including optical pulse propagation, quantum vortices in Bose-Einstein condensates (BECs), and plasma shock waves due to their properties of energy localization, waveform stability, and the capacity to retain their shape following collisions. Additionally, the dynamic equilibrium between nonlinear and dispersive terms allows solitons to achieve adaptive propagation in $(3+1)$-dimensional variable-coefficient systems [1–5]. A few of the fundamental methods for solving soliton solutions are the inverse scattering transform (IST) [6–8], the Darboux transformation (DT) [9–11], the Bäcklund transformation (BT) [12–14], the Hirota direct method [15–18] and so on. Among these, the Hirota bilinear method in conjunction with the long-wave limit [19–22] is a practical method for precisely resolving solutions to nonlinear evolution equations.

The Kadomtsev-Petviashvili (KP) equation [23], which has the following form:

$$(u_t + 6uu_x + u_{xxx})_x + au_{yy} = 0, \tag{1}$$

is constructed by generalizing the Korteweg-de Vries (KdV) equation to two spatial dimensions. Furthermore, numerous investigations have demonstrated that the KP equation may be used to help clarify the physical processes underlying nonlinear oscillations in BECs [24, 25] and to describe the nonlinear process of acoustic wave self-focusing and the two-dimensional dynamics of magnetic elastic solitons in antiferromagnets [26]. After substituting u_x for u in the KP equation, and integrating with respect to x, the potential Kadomtsev-Petviashvili (pKP) equation [18] is thus derived in the following form:

$$u_{xt} + 6u_x u_{xx} + u_{xxxx} + au_{yy} = 0. \tag{2}$$

This equation has been thoroughly examined in a number of areas since the solutions of the pKP equation were initially discovered [27] and appears in a number of important nonlinear problems in both mathematics and physics.

Additionally, the following is a representation of the $(2+1)$-dimensional integrable B-type Kadomtsev-Petviashvili (BKP) equation [28]:

$$\left(15(u_x)^3 + 15u_x u_{xxx} + u_{xxxxx}\right)_x + 5\left(u_{xxxy} + 3(u_x u_y)_x\right) + u_{xt} - u_{yy} = 0. \tag{3}$$

The high-dimensional characteristics of the BKP equation offer a wider range of waveforms for the modified KdV equation, including spiral waves and two-dimensional soliton chains. These waveforms can be used for fiber-optic communications and plasma physics signal transmission optimization. Furthermore, it provides mathematical tools for the analysis of complicated soliton structures due to its high-dimensional features and the balance between nonlinearity and dispersion. The pertinent results

have important ramifications for applications in nonlinear physics and engineering [29–35].

In 2021, Ma [36] introduced a combined version of the pKP and BKP equations, named as the pKP-BKP equation, which is expressed as follows:

$$\begin{aligned} &a_1\left(15(u_x)^3+15u_xu_{xxx}+u_{xxxxx}\right)_x+a_2(6u_xu_{xx}+u_{xxxx})\\ &+a_3\left(u_{xxxy}+3(u_xu_y)_x\right)+a_4u_{xx}+a_5u_{xt}+a_6u_{yy}=0, \end{aligned} \tag{4}$$

where a_i $(1\leq i\leq 6)$ are arbitrary constants with $a_5\neq 0$. Ma's work integrated the pKP equation and the BKP equation to create a high-dimensional integrable system, which analytically demonstrated the existence and dynamical behavior of N-soliton solutions using the Grassmann manifold approach, bilinear forms, and the Pfaffian structure of the BKP equation. This accomplishment offers a new paradigm for the study of multi-field coupled solitons and broadens the application bounds of the BKP equation in complicated nonlinear systems. For studies related to this new equation, one can refer to the following works [36–41]. Numerous researchers have been interested in the equation since it combines two integrability systems and has the dual effects of the pKP equation and the BKP equation [37]. Complex wave phenomena in high-dimensional nonlinear systems, such as the localized energy propagation in plasma or fluid mechanics, are described by the combined equation.

Recently, to build on previous achievements, Wazwaz [38] expanded Eq. (4) to a new $(3+1)$-dimensional combined pKP-BKP equation in order to improve on earlier successes, which is presented in the following form:

$$\begin{aligned} &u_{xt}+\alpha\left(15(u_x)^3+15u_xu_{xxx}+u_{xxxxx}\right)_x+\beta(6u_xu_{xx}+u_{xxxx})\\ &+\gamma\left(u_{xxxy}+3(u_xu_y)_x\right)+au_{xx}+bu_{xy}+cu_{xz}-\frac{\gamma^2}{5\alpha}u_{yy}=0. \end{aligned} \tag{5}$$

In this extension, additional terms, specifically bu_{xy} and cu_{xz}, are incorporated into the pKP-BKP equation, with a_5 set to 1, and $u=u(x,y,z,t)$. This newly combined pKP-BKP equation differs from Eq. (4) by including these new terms and extending it to the $(3+1)$-dimension. This paper mainly investigates the $(3+1)$-dimensional combined pKP-BKP equation, which methodically reveals the presence, stability, and interaction processes of lumps and multi-solitons in higher-dimensional space. Its conclusions give crucial mathematical tools for nonlinear wave management in multiphysical field coupling systems and broaden the theoretical bounds of integrable systems.

Solitons morphology and propagation trajectories can be actively controlled by varying the parameters of the equation, such as the dispersion coefficients and the nonlinear strength. This method offers guidelines for wave modification methods in domains such as energy transmission and optical communications. Furthermore, theoretical models for wave propagation in high-dimensional nonlinear systems, such

as inhomogeneous metamaterials and ocean wave systems, are established using the breather waves and Y-shaped soliton solutions obtained from these equations. These solutions provide crucial insights into intricate wave dynamics and nonlinear interactions and are especially useful for characterizing multidimensional energy localization and waveguiding events [39]. Until now, as far as we are aware, the soliton molecule of Eq. (5) has not been studied. Moreover, the lump solution of Eq. (5) has not been developed by the long-wave limit. The lump solution and the soliton molecule of the $(3+1)$-dimensional combined pKP-BKP equation (5) will be the main topics of this paper.

This paper is organized as follows. In Sec. 2, through the combination of the Hirota bilinear method and logarithmic transformation, we obtain the N-soliton and preliminarily derive the kink-shaped multi-soliton solutions of Eq. (5). The higher-order breathers and the mixed solutions of Eq. (5) are constructed based on different parameter relationships in Sec. 3. Section 4 constructs the soliton molecules of Eq. (5) by discussing and applying their resonance conditions on the (x,y)-, (y,z)-, and (x,z)-planes. In Sec. 5, the lump solutions of Eq. (5) are generated by taking the long wave limit. Section 6 introduces multiple varieties of semi-rational solutions of Eq. (5) and Sec. 7 gives the conclusions of this paper.

2. THE SOLITON SOLUTIONS OF THE NEW $(3+1)$-DIMENSIONAL COMBINED pKP-BKP EQUATION

Solitons, which are localized wave packets that preserve their waveform stability under the dynamic balance of dispersive and nonlinear forces, are the main focus of research in nonlinear integrable systems. Building on this basis, the N-soliton solution provides an accurate description of multi-soliton interactions, as evidenced by the soliton group's ability to transfer energy and momentum losslessly through phase shifts during elastic collisions while maintaining its initial propagation speeds, amplitudes, and waveform parameters. In this Section, the Hirota bilinear method, a significant tool renowned for its efficiency and powerful analytical capabilities in studying soliton solutions of nonlinear integrable systems, will be employed to systematically derive the N-soliton of Eq. (5). This approach effectively transforms the initially complicated nonlinear equation into a more manageable and understandable bilinear form by deftly utilizing the proper variable transformation strategies, offering a methodical way to build exact solutions. Our in-depth study and comprehension of the internal properties and solutions within nonlinear integrable systems are substantially aided by this transformation process. By performing the following logarithmic transformation

$$u = 2(\ln f)_x = 2\frac{f_x}{f}. \tag{6}$$

The relevant bilinear equation can be obtained by substituting this expression into Eq. (5) and carrying out a number of algebraic operations:

$$\left(D_xD_t+\alpha D_x^6+\beta D_x^4+\gamma D_x^3D_y+aD_x^2+bD_xD_y+cD_xD_z-\frac{\gamma^2}{5\alpha}D_y^2\right)f\cdot f=0, \tag{7}$$

where D is Hirota's bilinear derivative operator [15], and D_x^n and $D_t^mD_x^n$ are defined as

$$\begin{aligned} &D_x^n\,a\cdot b\equiv(\frac{\partial}{\partial x}-\frac{\partial}{\partial y})^n\,a(x)\,b(y)\mid_{y=x},\\ &D_t^mD_x^n\,a\cdot b\equiv\frac{\partial^m}{\partial s^m}\frac{\partial^n}{\partial y^n}a(t+s,x+y)\,b(t-s,x-y)\mid_{s=0,y=0}, \end{aligned} \tag{8}$$

where n and m are non-negative integers. The following is an expression for the equivalent bilinear expansion of Eq. (5):

$$\begin{aligned} &(ff_{xt}-f_xf_t)+\alpha\left(ff_{xxxxxx}-6f_xf_{xxxxx}+15f_{xx}f_{xxxx}-10(f_{xxx})^2\right)\\ &+\beta\left(ff_{xxxx}-4f_xf_{xxx}+3(f_{xx})^2\right)+\gamma(ff_{xxxy}-3f_xf_{xxy}+3f_{xx}f_{xy}-f_{xxx}f_y)\\ &+a(ff_{xx}-f_xf_x)+b(ff_{xy}-f_xf_y)+c(ff_{xz}-f_xf_z)-\frac{\gamma^2}{5\alpha}(ff_{yy}-f_yf_y)=0. \end{aligned} \tag{9}$$

Note that with regard to parameter ϵ, f can be extended into a series as

$$f=1+\epsilon f_1+\epsilon^2f_2+\cdots+\epsilon^kf_k+\cdots. \tag{10}$$

A comprehensive set of recurrence relations can be obtained by systematically gathering and organizing terms that share the same power of ϵ and substituting the expansion (10) into the bilinear equation Eq. (7):

$$\epsilon: f_{1,xt}+\alpha(f_{1,xxxxxx})+\beta(f_{1,xxxx})+\gamma(f_{1,xxxy})+af_{1,xx}+bf_{1,xy}+cf_{1,xz}-\frac{\gamma^2}{5\alpha}f_{1,yy}=0, \tag{11a}$$

$$\begin{aligned} &\epsilon^2: 2\left(f_{2,xt}+\alpha(f_{2,xxxxxx})+\beta(f_{2,xxxx})+\gamma(f_{2,xxxy})+af_{2,xx}+bf_{2,xy}+cf_{2,xz}-\frac{\gamma^2}{5\alpha}f_{2,yy}\right)\\ &=-\left(D_xD_t+\alpha D_x^6+\beta D_x^4+\gamma D_x^3D_y+aD_x^2+bD_xD_y+cD_xD_z-\frac{\gamma^2}{5\alpha}D_y^2\right)f_1\cdot f_1, \end{aligned} \tag{11b}$$

$$\begin{aligned} &\epsilon^3: f_{3,xt}+\alpha(f_{3,xxxxxx})+\beta(f_{3,xxxx})+\gamma(f_{3,xxxy})+af_{3,xx}+bf_{3,xy}+cf_{3,xz}-\frac{\gamma^2}{5\alpha}f_{3,yy}\\ &=-\left(D_xD_t+\alpha D_x^6+\beta D_x^4+\gamma D_x^3D_y+aD_x^2+bD_xD_y+cD_xD_z-\frac{\gamma^2}{5\alpha}D_y^2\right)f_1\cdot f_2, \end{aligned} \tag{11c}$$

$\cdots$.

In exponential form, let f_1 be a pure virtual function, then $f_2 = f_3 = f_4 = \cdots = 0$ and hence f can be presented in the following form

$$f(x,y,z,t) = 1 + \epsilon f_1, \tag{12}$$

where

$$\begin{aligned} &f_1 = e^{\psi_1}, \\ &\psi_1 = p_1 x + q_1 y + k_1 z + w_1 t + \psi_1^{(0)}, \\ &w_1 = -\frac{\alpha p_1^6 + \beta p_1^4 + \gamma p_1^3 q_1 + a p_1^2 + b p_1 q_1 + c p_1 k_1 - \frac{\gamma^2}{5\alpha} q_1^2}{p_1}. \end{aligned} \tag{13}$$

Here, $-w_1$ is the frequency, $\psi_1^{(0)}$ is the phase constant and the wavenumber components along the x, y, and z directions are represented by p_1, q_1, and k_1, respectively. These parameters need to satisfy the $(3+1)$-dimensional dispersion relation determined by the first-order terms of the bilinear equation. Meanwhile, using the transformation (6) and let $\epsilon = 1$, then the single-soliton solution of Eq. (5) may be represented as

$$u_{1s} = \frac{2p_1 e^{\psi_1}}{1 + e^{\psi_1}} = \frac{2p_1}{1 + e^{-p_1 x + q_1 y + k_1 z + w_1 t + \psi_1^{(0)}}}. \tag{14}$$

We review some basic facts about u_{1s}. Firstly, u_{1s} has no extreme point and the position of the soliton is often represented by the parameter $\psi_1^{(0)}$, which is set to 0. Moreover, we have the following:

$$\begin{cases} u_{1s} \to 2p_1 & \text{as} \quad \psi_1 \to +\infty \\ u_{1s} \to 0 & \text{as} \quad \psi_1 \to -\infty. \end{cases} \tag{15}$$

The most crucial part of researching the 1-soliton solution u_{1s} is comprehending the asymptotic dynamic characteristic. When p_1=0, u_{1s} will transform into a plane wave. On the other hand, if $p_i \neq 0$, u_{1s} will transform into a kink wave. Recall that a kink wave represents a class of nonlinear localized waves exhibiting a topological feature, characterized by a spatial phase jump (typically π radians) in their waveform profiles during propagation. When all parameters are given specific values in (14), a 1-kink wave is generated with specific parameters in Fig. 1(a).

The linear superposition approach, a method that makes solving complex problems significantly simpler, can provide a superposition solution of Eq. (11a):

$$f_1 = e^{\psi_1} + e^{\psi_2}, \tag{16}$$

where

$$\begin{aligned}
&\psi_l = p_l x + q_l y + k_l z + w_l t + \psi_l^{(0)}, \\
&w_l = -\frac{\alpha p_l^6 + \beta p_l^4 + \gamma p_l^3 q_l + a p_l^2 + b p_l q_l + c p_l k_l - \frac{\gamma^2}{5\alpha} q_l^2}{p_l} \qquad (l = 1, 2).
\end{aligned} \tag{17}$$

Substituting Eq. (16) into Eq. (11b), we obtain the following:

$$f_2 = e^{\psi_1 + \psi_2 + A_{12}}, \tag{18}$$

where

$$\begin{aligned}
&e^{A_{12}} = \frac{A^2\left((p_1^2 - p_1 p_2 + p_2^2) + \frac{3\beta}{5\alpha}\right) + A\gamma(p_1^2 q_2 + 2p_1 p_2 q_1 - 2p_{l1} p_2 q_2 - p_2^2 q_1) + C}{B^2\left((p_1^2 + p_1 p_2 + p_2^2) + \frac{3\beta}{5\alpha}\right) + B\gamma(p_1^2 q_2 + 2p_1 p_2 q_1 + 2p_1 p_2 q_2 + p_2^2 q_1) + C}, \\
&A = 5\alpha p_1 p_2 (p_1 - p_2), \\
&B = 5\alpha p_1 p_2 (p_1 + p_2), \\
&C = \gamma^2 (p_1 q_2 - p_2 q_1)^2.
\end{aligned} \tag{19}$$

Similarly, it is possible to express the truncated solution of Eq. (7) using the perturbation method once more as

$$f_2(x, y, z, t) = 1 + e^{\psi_1 + \psi_2 + A_{12}} + e^{\psi_1} + e^{\psi_2}. \tag{20}$$

Thus, combined the above transformation (6), the 2-soliton solution of Eq. (5) will take the following formulation:

$$u_{2s} = 2[\ln(1 + e^{\psi_1 + \psi_2 + A_{12}} + e^{\psi_1} + e^{\psi_2})]_x. \tag{21}$$

The three-soliton solution of Eq. (5) can be found by following the equivalent procedure described above:

$$\begin{aligned}
u_{3s} = 2[\ln(1 + e^{\psi_1} + e^{\psi_2} + e^{\psi_3} + e^{\psi_1 + \psi_2 + A_{12}} + e^{\psi_1 + \psi_3 + A_{13}} \\
+ e^{\psi_2 + \psi_3 + A_{23}} + e^{\psi_1 + \psi_2 + \psi_3 + A_{12} + A_{13} + A_{23}})]_x,
\end{aligned} \tag{22}$$

where

$$
\begin{aligned}
&\psi_l = p_l x + q_l y + k_l z + w_l t + \psi_l^{(0)},\\
&w_l = -\frac{\alpha p_l^6 + \beta p_l^4 + \gamma p_l^3 q_l + a p_l^2 + b p_l q_l + c p_l k_l - \frac{\gamma^2}{5\alpha} q_l^2}{p_l},\\
&e^{A_{lj}} = \frac{A^2\left((p_l^2 - p_l p_j + p_j^2) + \frac{3\beta}{5\alpha}\right) + A\gamma(p_l^2 q_j + 2p_l p_j q_l - 2p_l p_j q_j - p_j^2 q_l) + C}{B^2\left((p_l^2 + p_l p_j + p_j^2) + \frac{3\beta}{5\alpha}\right) + B\gamma(p_l^2 q_j + 2p_l p_j q_l + 2p_l p_j q_j + p_j^2 q_l) + C},\\
&A = 5\alpha p_l p_j (p_l - p_j),\\
&B = 5\alpha p_l p_j (p_l + p_j),\\
&C = \gamma^2 (p_l q_j - p_j q_l)^2,\\
&(1 \le l < j \le 3).
\end{aligned}
\tag{23}
$$

It turns out that kink waves are actually a type of traveling waves. Through enabling certain parameters, Figs. 1(b), (c), and (d) depict the dynamic properties of 2-, 3-, and 4-kink soliton solutions.

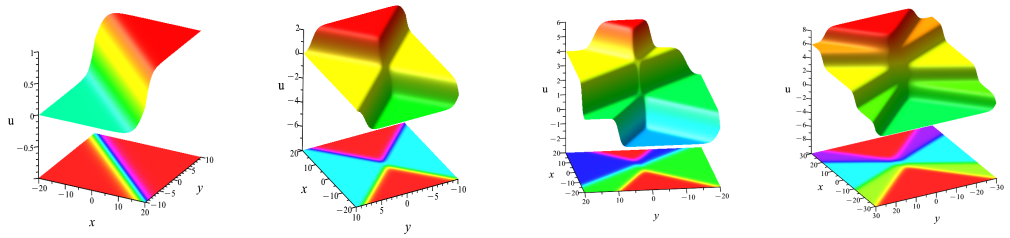

(a) $t = 0$ (b) $t = 0$ (c) $t = 0$ (d) $t = 0$

Fig. 1 – (Color online) (a) 1-kink wave (14) with $a = b = c = \alpha = \beta = 1, \gamma = 3, p_1 = 0.5, q_1 = 1, k_1 = 1, \psi_1^0 = 0$; (b) 2-kink wave (21) with $a = b = c = \alpha = \beta = \gamma = 1, p_1 = -p_2 = k_1 = k_2 = 1, q_1 = q_2 = 2, \psi_1^0 = \psi_2^0 = 0$; (c) 3-kink wave (22) with $a = b = c = \alpha = \beta = \gamma = 1, p_1 = p_2 = p_3 = q_1 = -q_3 = k_1 = k_2 = k_3 = 1, q_2 = 2, \psi_1^0 = \psi_2^0 = \psi_3^0 = 0$; (d) 4-kink wave of Eq. (5) with $a = b = c = \alpha = \beta = 1, \gamma = 5, p_1 = k_1 = p_2 = k_2 = p_3 = -q_3 = k_3 = p_4 = q_4 = k_4 = 1, q_1 = -q_2 = 0.5, \psi_1^0 = \psi_2^0 = \psi_3^0 = \psi_4^0 = 0$.

By repeating the above method all the time, we can get the N-soliton solutions of Eq. (5) as follows [38]:

$$
\begin{aligned}
u &= 2(\ln f)_x\\
&= 2\left[\ln\left(\sum_{\mu=0,1} e^{\sum_{l=1}^{N}\mu_l\psi_l + \sum_{1\le l<j}^{N}\mu_l\mu_j A_{lj}}\right)\right]_x,
\end{aligned}
\tag{24}
$$

where

$$
\begin{aligned}
&\psi_l = p_l x + q_l y + k_l z + w_l t + \psi_l^{(0)},\\
&w_l = -\frac{\alpha p_l^6 + \beta p_l^4 + \gamma p_l^3 q_l + a p_l^2 + b p_l q_l + c p_l k_l - \frac{\gamma^2}{5\alpha} q_l^2}{p_l},\\
&e^{A_{lj}} = \frac{A^2\left((p_l^2 - p_l p_j + p_j^2) + \frac{3\beta}{5\alpha}\right) + A\gamma(p_l^2 q_j + 2p_l p_j q_l - 2p_l p_j q_j - p_j^2 q_l) + C}{B^2\left((p_l^2 + p_l p_j + p_j^2) + \frac{3\beta}{5\alpha}\right) + B\gamma(p_l^2 q_j + 2p_l p_j q_l + 2p_l p_j q_j + p_j^2 q_l) + C},\\
&A = 5\alpha p_l p_j (p_l - p_j),\\
&B = 5\alpha p_l p_j (p_l + p_j),\\
&C = \gamma^2 (p_l q_j - p_j q_l)^2,\\
&(l < j, \quad l, j = 1, 2, \ldots, N).
\end{aligned}
\tag{25}
$$

It is worth noting that these parameters $p_l, q_l, \psi_l^{(0)}$ can only take complex or real numbers. The above summation symbol $\mu = 0, 1$ behind the logarithmic sign should be any potential pairings of $\mu_i = 0, 1$ $(i = 1, 2, \ldots, N)$. Otherwise, the nonlinear dispersion relation of Eq. (5) is represented by

$$
w_l + \frac{\alpha p_l^6 + \beta p_l^4 + \gamma p_l^3 q_l + a p_l^2 + b p_l q_l + c p_l k_l - \frac{\gamma^2}{5\alpha} q_l^2}{p_l} = 0.
$$

This is an important component that significantly affects the many other rich solutions obtained from Eq. (5). It is especially noticeable in terms of the locality and periodicity of the energy distribution.

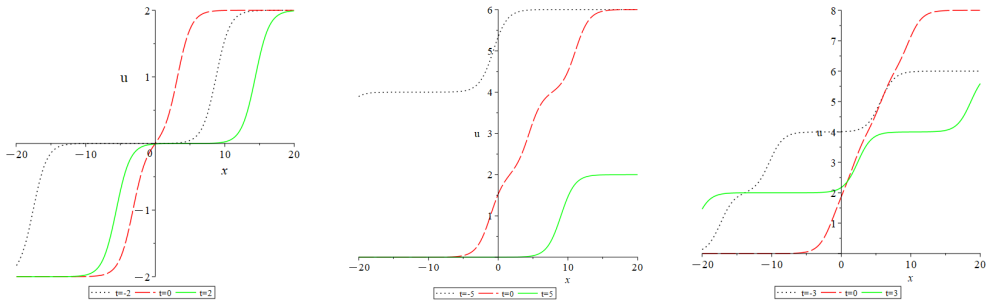

(a) $y = 0, z = 0$ (b) $y = 0, z = 0$ (c) $y = 0, z = 0$

Fig. 2 – (Color online) Dynamic evolution graph in two-dimensions with $z = 0$ and $y = 0$. (a) 2-kink wave (21) with $a = b = c = \alpha = \beta = \gamma = 1, p_1 = -p_2 = k_1 = k_2 = 1, q_1 = q_2 = 2, \psi_1^0 = \psi_2^0 = 0$; (b) 3-kink wave (22) with $a = b = c = \alpha = \beta = \gamma = 1, p_1 = p_2 = p_3 = q_1 = -q_3 = k_1 = k_2 = k_3 = 1, q_2 = 2, \psi_1^0 = \psi_2^0 = \psi_3^0 = 0$; (c) 4-kink wave of Eq. (5) with $a = b = c = \alpha = \beta = 1, \gamma = 5, p_1 = k_1 = p_2 = k_2 = p_3 = -q_3 = k_3 = p_4 = q_4 = k_4 = 1, q_1 = -q_2 = 0.5, \psi_1^0 = \psi_2^0 = \psi_3^0 = \psi_4^0 = 0$.

We analyzed the shape characteristics of 1-, 2-, 3-, and 4-soliton solutions and their twisted waveforms. By varying the parameters and observing the changes in the soliton solutions, it is possible to ascertain that the existence of twisted features is dependent on $p_i \neq 0 (i = 1, 2, 3, 4)$. Furthermore, the value of p_i also affects the shape characteristics of multi-soliton solutions, highlighting their diversity. Solitary waves demonstrate particle-like structure and their propagation can be visually understood from these graphs. Due to the interaction and influence between nonlinear effects and dispersion phenomena, solitary waves exhibit elastic properties during their collisions with each other, allowing for changes in phase but prohibiting changes in shape, size (velocity), and direction. And the interrelations among these solitons with kink shapes cause the amplitudes in their intersecting areas to exhibit a temporary abnormality (see Figs. 1 and 2).

3. THE BREATHER SOLUTIONS OF THE NEW $(3+1)$-DIMENSIONAL COMBINED pKP-BKP EQUATION

As a family of confined wave structures in nonlinear physical systems, breathers maintain spatial waveform localization while displaying periodic amplitude oscillations throughout the temporal dimension. Breathers exhibit special elastic collision features in multi-soliton collisions: dynamical evolution is accomplished only by phase shifts, while energy and momentum are conserved. The modulation effect of multi-soliton solutions on breather dynamics is the source of this periodic oscillatory behavior. Because multi-soliton solutions are essentially produced by exponential functions, new hybrid solutions with composite properties can be created by combining them with breather solutions. In addition to examining the various morphological forms of breathers, the current research emphasizes their potential for cross-disciplinary applications, from coherent control in quantum simulations to signal modulation in optical communications, which promotes continuous convergence. Different breather solutions will be analyzed in this Section by controlling the parameters in Eq. (24) and the parameter (25) through complex conjugate constraints. Let

$$N = 2n, \quad p_{2l} = p^*_{2l-1}, \quad q_{2l} = q^*_{2l-1}, \quad k_{2l} = k^*_{2l-1}, \quad \psi^0_{2l} = \psi^{0*}_{2l-1}, \tag{26}$$

where $l = 1, 2, 3, \ldots, n$ and n is a positive integer. For the purpose of obtaining the 1-breather solution, we take $N = 2, a = b = c = \alpha = \beta = \gamma = 1, p_1 = p^*_2 = k_1 = k^*_2 = i, q_1 = q^*_2 = 3 - i, \psi^0_1 = \psi^0_2 = 0$, and the formula (21) can be rewritten as

$$u_{1b} = \frac{-2ie^{\delta} + 2ie^{\delta^*}}{1 + e^{\delta} + e^{\delta^*} - \frac{22}{3}e^{\zeta}}, \tag{27}$$

where

$$\begin{aligned}\delta &= -(\frac{6}{5}+\frac{18}{5}i)t+ix+(3-i)y-iz,\\ \zeta &= -\frac{12}{5}t+6y.\end{aligned} \tag{28}$$

The 1-breather solutions are displayed in Fig. 3.

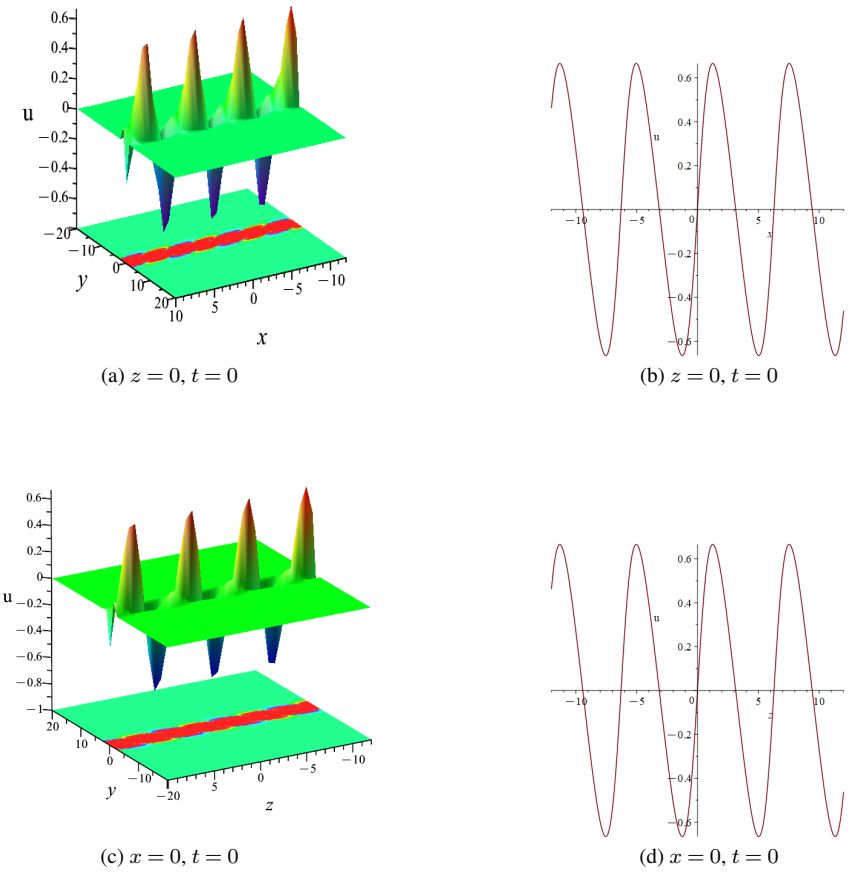

(a) $z=0, t=0$ (b) $z=0, t=0$

(c) $x=0, t=0$ (d) $x=0, t=0$

Fig. 3 – (Color online) The 1-breather solution (27) with $a=b=c=\alpha=\beta=\gamma=1, p_1=p_2^*=k_1=k_2^*=i, q_1=q_2^*=3-i, \psi_1^0=\psi_2^0=0$.

The 1-breather solution u_{1b} (27) exhibits a periodic motion orbital on the x-axis (see Figs. 3(a) and (b)) for an observation. When $x=0$, u_{1b} (27) exhibits a periodic motion orbital on the z-axis (see Figs. 3(c) and (d)). When $y=0$, Fig. 4 illustrates a periodic line wave that fluctuates in an up-and-down motion over time. While the density plots at $t=-2$, $t=0$ and $t=5$ appear similar, the z-axis reveals that one

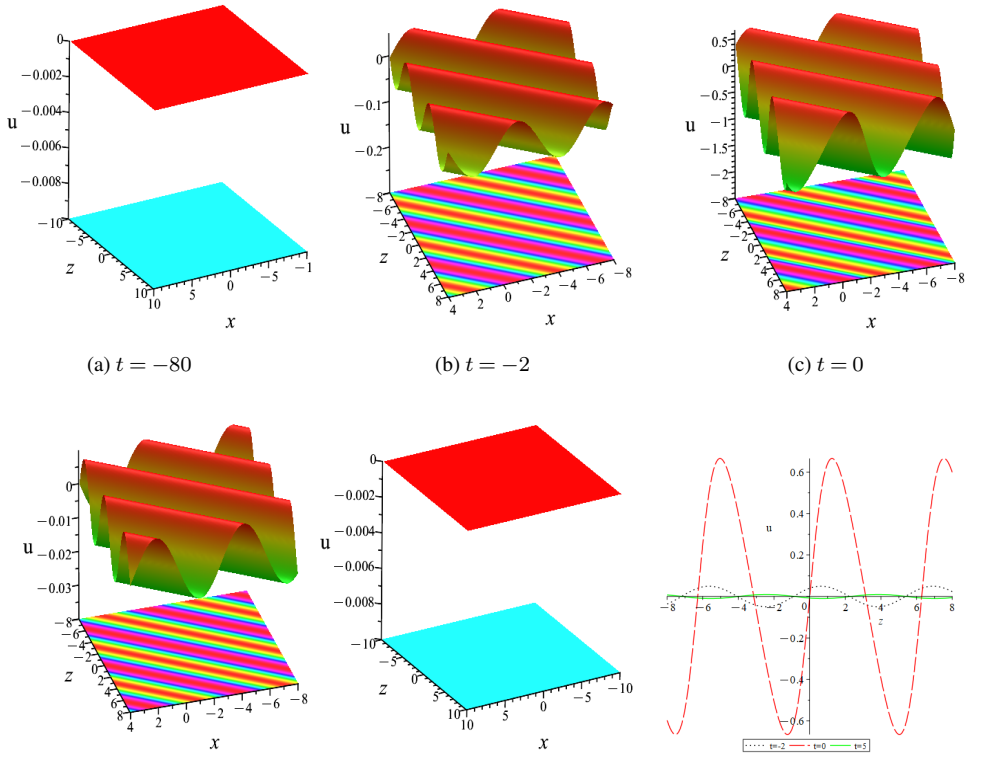

(a) $t=-80$ (b) $t=-2$ (c) $t=0$

(d) $t=5$ (e) $t=50$ (f) $x=0$

Fig. 4 – (Color online) First-order periodic solution (27) with $a=b=c=\alpha=\beta=\gamma=1, p_1=p_2^*=k_1=k_2^*=i, q_1=q_2^*=3-i, \psi_1^0=\psi_2^0=0$ at $y=0$.

notable feature of this particular periodic linear wave is that it decays steadily over a very short period of time until it eventually vanishes entirely, or decays to zero. Subsequent analysis shows that the greatest amplitude of this waveform happens exactly when $t=0$.

To obtain the higher-order solution, we take $N=4, a=b=c=\alpha=\beta=\gamma=1, p_1=p_2^*=k_1=k_2^*=-2i, q_1=q_2^*=1+i, \psi_1^0=\psi_2^0=\pi, p_3=p_4^*=k_3=k_4^*=-2i, q_3=q_4^*=1-i, \psi_3^0=\psi_4^0=-\pi$ in Eqs. (24) and (25). Figure 5 shows the situation of 2-breather solutions. The 2-breather solution is similar to the first-order one in that both of them show periodicity.

For $N\geq 3$, the n-order breather and m-order soliton mixed solutions can be constructed. For instance, the mixed solution combining the 1-kink solution and the 1-breather solution (see Fig. 6(a)) can be generated by taking $N=3, a=b=c=\alpha=\beta=1, \gamma=5, p_1=q_1=k_1=1, p_2=k_2=q_2^*=1+i, p_3=k_3=q_3^*=1-i, \psi_1^0=\psi_2^0=\psi_3^0=0$.

Thus, the mixed solution combining the 1-kink solution and the 1-breather solution take the following form:

$$u_{1b-1s}=2\frac{e^{\eta_1}+(1+i)e^{\nu_1}+(1-i)e^{\nu_1^*}+\delta_1 e^{\nu_1+\nu_1^*}+\delta_1^* e^{\nu_1+\nu_1^*}+\frac{14e^{\phi_1}}{13}+\frac{2289e^{\phi_2}}{182845}}{1+e^{\psi_1}+e^{\nu_1}+e^{\nu_1^*}+\lambda_1 e^{\nu_1+\nu_1^*}+\lambda_1^* e^{\nu_1+\nu_1^*}+\frac{7e^{\phi_1}}{13}+\frac{763e^{\phi_2}}{182845}}, \tag{29}$$

where

$$\begin{aligned}
&\eta_1=-5t+x+y+z,\\
&\nu_1=-(12+14i)t+(1+i)x+(1-i)y+(1+i)z,\\
&\delta_1=\frac{256}{2813}+\frac{491i}{2813},\\
&\phi_1=-24t+2x+2y+2z,\\
&\phi_2=-29t+3x+3y+3z.
\end{aligned} \tag{30}$$

The 1-breather solution of Eq. (5) retains its distinctive periodic behavior, going through frequent and recurring changes, irrespective of how these two types of solutions interact or clash. This discovery highlights the periodic qualities of the 1-breather solution's stability and robustness, which are unaffected by interactions with other solutions or external perturbations.

Using the same method, it is possible to construct the combined solution by integrating the 1-breather solution and the 2-kink soliton solution by taking the parameters $N=4, a=b=c=\beta=1, \alpha=2, \gamma=5, p_1=q_3=k_1=1+i, p_2=q_2=q_4=1, p_3=q_1=k_3=1-i, p_4=k_2=k_4=-1, \psi_1^0=\psi_2^0=\psi_3^0=\psi_4^0=0$. We can see the specific characteristic status of the mixed solution combining the 1-breather solution and the 2-kink soliton solution in Fig. 6(b). One feature that stands out of the physical consequences of these mixed solutions is that the clash between the breather solutions and the 2-kink soliton solutions of Eq. (5) does not influence the periodicity or localization of the breather solutions on the (x,y)-plane. What is more, the waveform properties of the breathers are "locked" without deformation or distortion, precisely maintaining their waveform state from the beginning moment, regardless of the propagation distance or changes in the propagation environment.

4. THE SOLITON MOLECULES OF THE NEW $(3+1)$-DIMENSIONAL COMBINED pKP-BKP EQUATION

Similar to molecular structures in chemistry, soliton molecules are stable bound states created by many solitons through nonlinear interactions. The processes of solitons' attraction, repulsion or phase locking determine how they arise. The profound mechanisms of energy localization in many-body systems are revealed by soliton molecules, a characteristic phenomenon in nonlinear science and their research has both great technical application value and fundamental physics significance. For

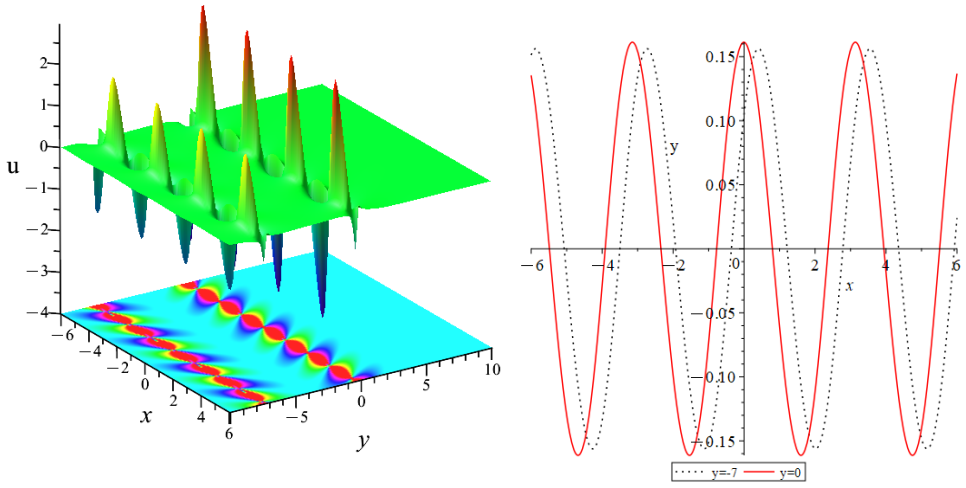

(a) $z=0, t=0$ (b) $z=0, t=0$

Fig. 5 – (Color online) 2-breather solution with $a=b=c=\alpha=\beta=\gamma=1, p_1=p_2^*=p_3=p_4^*=-2i, q_1=q_2^*=q_4=q_3^*=1+i, k_1=k_2^*=k_3=k_4^*=-i, \psi_1^0=\psi_2^0=\pi, \psi_3^0=\psi_4^0=-\pi$.

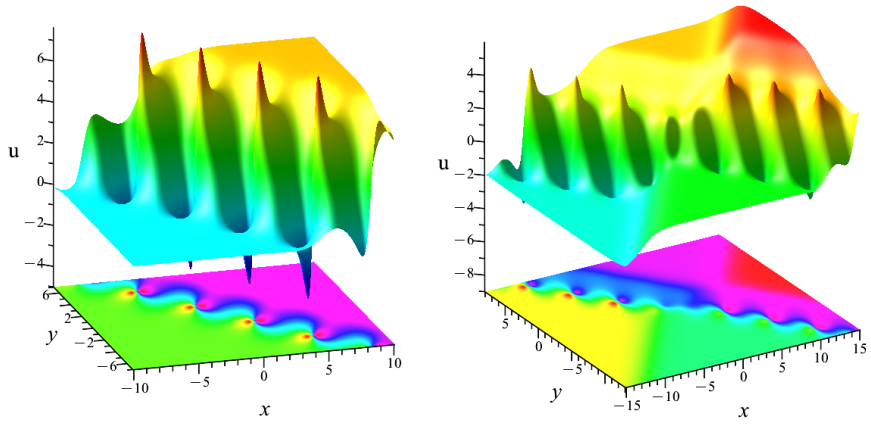

(a) $t=0$ (b) $t=0$

Fig. 6 – (Color online) (a) The mixed solution of 1-kink solution and the 1-breather solution (29) with $a=b=c=\alpha=\beta=1, \gamma=5, p_1=q_1=k_1=1, p_2=k_2=q_2^*=1+i, p_3=k_3=q_3^*=1-i, \psi_1^0=\psi_2^0=\psi_3^0=0$. (b) The mixed solution of 2-kink solution and the 1-breather solution with $a=b=c=\beta=1, \alpha=2, \gamma=5, p_1=q_3=k_1=1+i, p_2=q_2=q_4=1, p_3=q_1=k_3=1-i, p_4=k_2=k_4=-1, \psi_1^0=\psi_2^0=\psi_3^0=\psi_4^0=0$.

instance, by manipulating chemical states, soliton molecules can be utilized for optical signal encoding, which allows multi-bit information to be stored and sent. While the dynamical similarity offers a new model for investigating the nonequilibrium evolution of correlated electron systems, the soliton molecule analogy based on nonlinear interactions creates an interdisciplinary bridge for quantum material design in condensed matter physics and many-body dynamics research in quantum simulation. Therefore, soliton molecules have drawn significant attention in multiple areas, including optical systems [5, 42–44].

Many theoretical models for the formation of soliton molecules have been put forward. The two main components of the soliton molecule production mechanism are dynamical evolution and interaction regulation. Using Feshbach resonance techniques, which can change repulsive interactions into attractive ones, the interaction management is accomplished by varying the scattering length between atoms. When the interactions of two solitons dominate the dynamical behavior and their phase difference and spacing meet specific criteria, a stable bound state and a soliton molecule are created. In the dynamical evolution process, the initial solitons exchange energy through nonlinear interactions during their propagation, undergoing a dynamic equilibrium between attraction and repulsion and finally stabilizing into a molecular state under certain parametric circumstances [45, 46]. A wide range of integrable systems can be studied using the resonant theory of solitons. When different resonance conditions are imposed on the N-soltion solutions (24), many types of soliton molecules can be constructed on different planes [47, 48].

Case 1: The resonance condition on the (x, y)-plane is:

$$\frac{p_i}{p_j} = \frac{q_i}{q_j} \tag{31}$$

which gives

$$p_i = \frac{q_i p_j}{q_j}. \tag{32}$$

On the (x, y)-plane, the soliton molecules can subsequently be obtained through taking formula (32) into Eq. (24) and Eq. (25).

Case 2: The resonance condition on the (x, z)-plane is:

$$\frac{p_i}{p_j} = \frac{k_i}{k_j} \tag{33}$$

which leads to

$$p_i = \frac{p_j k_i}{k_j}. \tag{34}$$

Similarly, on the (x, z)-plane, the soliton molecules can subsequently be obtained through taking formula (34) into Eq. (24) and Eq. (25).

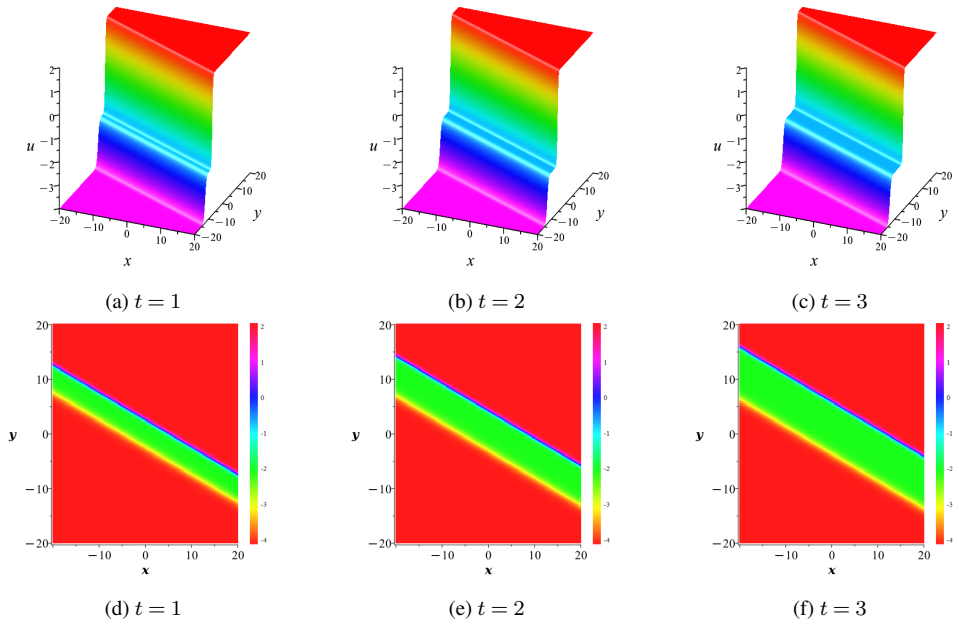

(a) $t = 1$ (b) $t = 2$ (c) $t = 3$

(d) $t = 1$ (e) $t = 2$ (f) $t = 3$

Fig. 7 – (Color online) Description of the soliton molecule with 2-soliton on the (x, y)-plane.

Case 3: The resonance condition on the (y, z)-plane is:

$$\frac{q_i}{q_j} = \frac{k_i}{k_j} \tag{35}$$

which gives

$$q_i = \frac{q_j k_i}{k_j}. \tag{36}$$

Thus, on the (y, z)-plane, the soliton molecules can subsequently be obtained through taking formula (36) into Eq. (24) and Eq. (25).

Figure 7 depicts the diagram of soliton molecule configuration of Eq. (5) with $N = 2$, where the parameters have been specifically chosen as:

$$\begin{cases} a = b = c = \alpha = \beta = 1, \gamma = -2 \\ p_1 = 1, q_1 = 2, k_1 = 1, \psi_1^0 = 0 \\ p_2 = -2, q_2 = -4, k_2 = 1, \psi_2^0 = 0. \end{cases} \tag{37}$$

Figure 7 displays the properties of the soliton molecule with 2-soliton for various times on the (x, y)-plane. It is evident that the two solitons are parallel to one another and are moving at the equivalent speed.

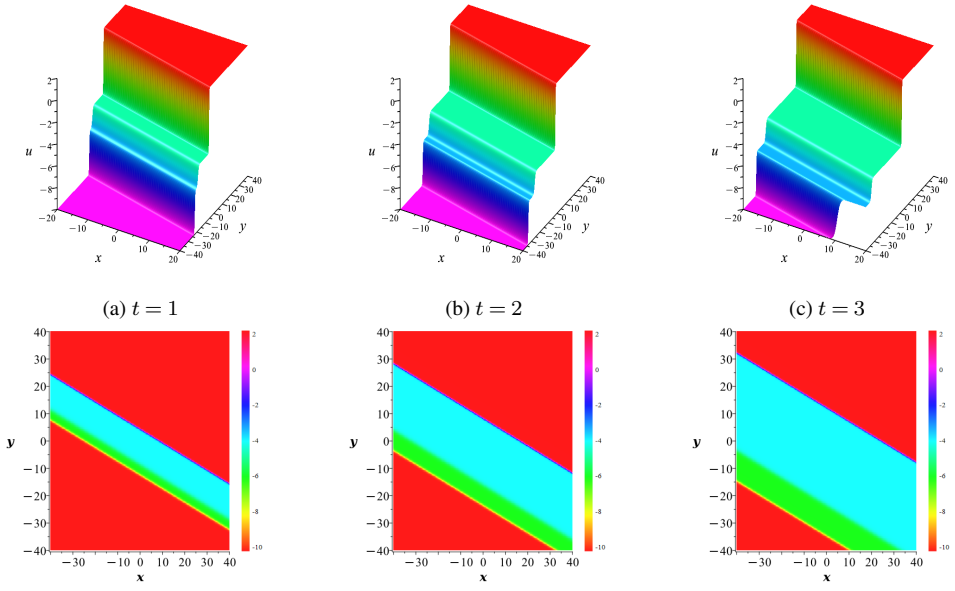

(a) $t = 1$ (b) $t = 2$ (c) $t = 3$

(d) $t = 1$ (e) $t = 2$ (f) $t = 3$

Fig. 8 – (Color online) Description of the soliton molecule with 3-soliton on the (x, y)-plane.

We utilize the parameters as follows for $N = 3$:

$$\begin{cases} a = b = c = \alpha = \beta = 1, \gamma = -4 \\ p_1 = 1, q_1 = 2, k_1 = 1, \psi_1^0 = 0 \\ p_2 = -2, q_2 = -4, k_2 = 1, \psi_2^0 = 0 \\ p_3 = -3, q_3 = -6, k_3 = 1, \psi_3^0 = 0. \end{cases} \tag{38}$$

Similarly, Fig. 8 displays the properties of the soliton molecule with 3-soliton for various times on the (x, y)-plane. Furthermore, over time, they move separately and avoid any mutual interference.

For the soliton molecule with 4-soliton when N = 4, let us choose the following parameters:

$$\begin{cases} a = b = c = \alpha = \beta = 1, \gamma = -8 \\ p_1 = 0.5, q_1 = 1, k_1 = 1, \psi_1^0 = 0 \\ p_2 = -1, q_2 = -2, k_2 = 1, \psi_2^0 = 0 \\ p_3 = -2, q_3 = -4, k_3 = 1, \psi_3^0 = 0 \\ p_4 = -3, q_4 = -6, k_4 = 1, \psi_4^0 = 0. \end{cases} \tag{39}$$

Analogously, Fig. 9 displays the properties of the soliton molecule with 4-soliton for various times on the (x, y)-plane. Hereby the four solitons are all parallel

to each other and there is no intersection among them.

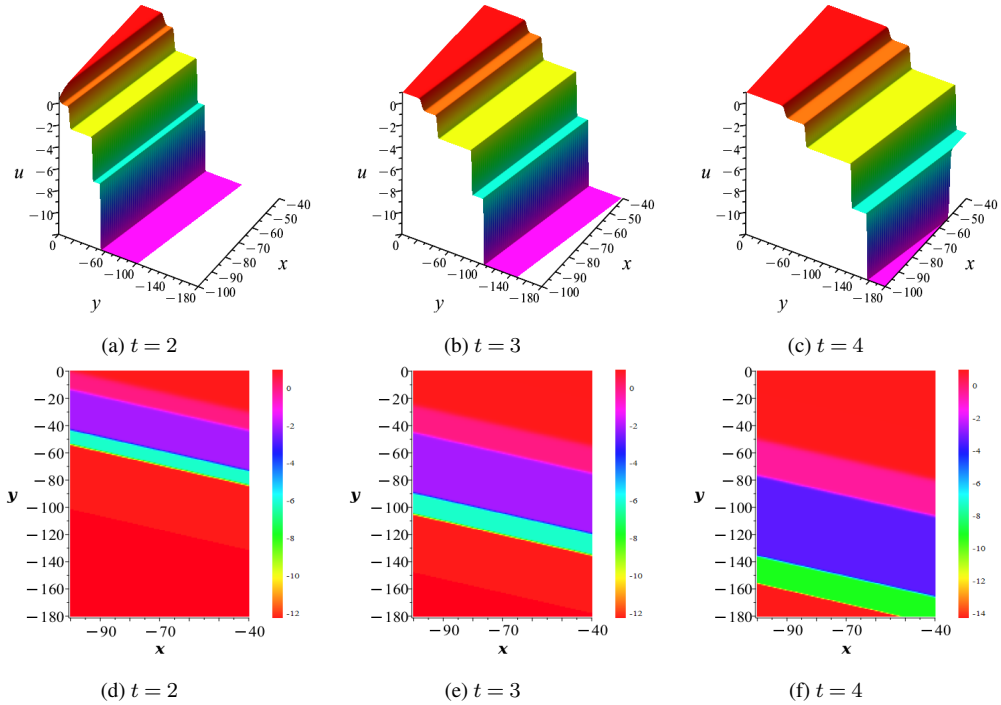

(a) $t = 2$ (b) $t = 3$ (c) $t = 4$

(d) $t = 2$ (e) $t = 3$ (f) $t = 4$

Fig. 9 – (Color online) Description of the soliton molecule with 4-soliton on the (x, y)-plane.

Then, we will seek out some mixed interaction solutions of Eq. (5). By permitting the solitons to meet the resonance criterion, we can create the 1-soliton and the 1-soliton molecule for $N = 3$. Here, we select the following parameters:

$$\begin{cases} a = b = c = \alpha = \beta = 1, \gamma = -6 \\ p_1 = 1, q_1 = 2, k_1 = 1, \psi_1^0 = 0 \\ p_2 = -2, q_2 = -4, k_2 = 1, \psi_2^0 = 0 \\ p_3 = 1, q_3 = -1, k_3 = 1, \psi_3^0 = 0. \end{cases} \tag{40}$$

Figure 10 illustrates the dynamic interplay among the 1-soliton and the 1-soliton molecule on the (x, y)-plane for various times. As time progresses, both the soliton molecule and the 1-soliton are propagating the negative directions of the $x-$ and $y-$axis, and their collision turns out to be elastic.

We can create three distinct interactions for $N = 4$ by letting

(1) the resonance condition, a prerequisite for stable soliton interactions, is met by the two-soliton,

(2) the resonance condition, a prerequisite for stable soliton interactions, is met by the

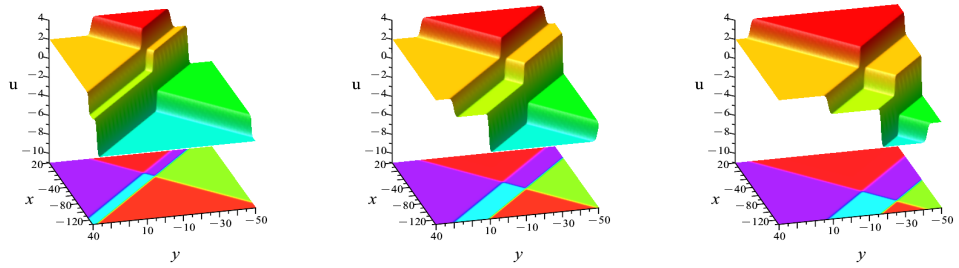

(a) $t = 1$ (b) $t = 2$ (c) $t = 3$

Fig. 10 – (Color online) Description of the dynamic interplay among the 1-soliton and the 1-soliton molecule on the (x, y)-plane when $z = 0$.

three-soliton,
(3) the resonance condition, a prerequisite for stable soliton interactions, is met by the two and the other two-soliton.
Case 1: Figure 11(a) uses the following parameters to depict the interaction among the 2-soliton and the 1-soliton molecule on the (x, y)-plane when $t = 2, z = 0$:

$$\begin{cases} a = b = c = \alpha = \beta = 1, \gamma = -4 \\ p_1 = 0.5, q_1 = 1, k_1 = 1, \psi_1^0 = 0 \\ p_2 = -1, q_2 = -2, k_2 = 1, \psi_2^0 = 0 \\ p_3 = 1, q_3 = -2, k_3 = 1, \psi_3^0 = 0 \\ p_4 = 1, q_4 = -1, k_4 = 1, \psi_4^0 = 0. \end{cases} \tag{41}$$

Case 2: Figure 11(b) can depict the dynamic interplay among the 1-soliton and the 2-soliton molecule on the (x, y)-plane, by fixing the parameters as:

$$\begin{cases} a = b = c = \alpha = \beta = 1, \gamma = -6 \\ p_1 = 0.5, q_1 = 1, k_1 = 1, \psi_1^0 = 0 \\ p_2 = -2, q_2 = -4, k_2 = 1, \psi_2^0 = 0 \\ p_3 = -3, q_3 = -6, k_3 = 1, \psi_3^0 = 0 \\ p_4 = 1, q_4 = -2, k_4 = 1, \psi_4^0 = 0. \end{cases} \tag{42}$$

Case 3: Figure 11(c) selects the following parameters to show the dynamic interplay among the 1-soliton molecule and the 1-soliton molecule on the (x, y)-plane

$$\begin{cases} a = b = c = \alpha = \beta = 1, \gamma = -7 \\ p_1 = 0.5, q_1 = 1, k_1 = 1, \psi_1^0 = 0 \\ p_2 = -2, q_2 = -4, k_2 = 1, \psi_2^0 = 0 \\ p_3 = -1, q_3 = 2, k_3 = 1, \psi_3^0 = 0 \\ p_4 = -2, q_4 = 4, k_4 = 1, \psi_4^0 = 0. \end{cases} \tag{43}$$

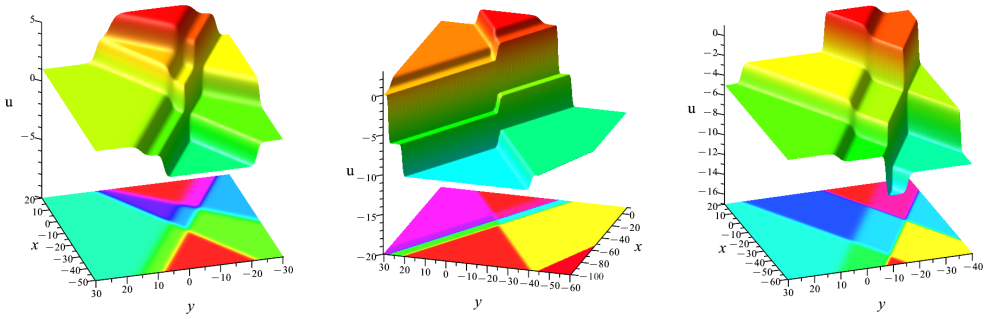

(a) $t = 2$ (b) $t = 1$ (c) $t = 1$

Fig. 11 – (Color online) (a) Description of the dynamic interplay among the 2-soliton and the 1-soliton molecule on the (x, y)-plane when $z = 0$, $t = 2$. (b) Description of the dynamic interplay among the 1-soliton and the 2-soliton molecule on the (x, y)-plane when $z = 0$, $t = 1$. (c) Description of the dynamic interplay among the 1-soliton molecule and 1-soliton molecule on the (x, y)-plane when $z = 0$, $t = 1$.

It is possible to clearly identify the key features of soliton molecules by carefully examining the pictures in this Section. In particular, during the propagation process, the individual solitons that comprise a soliton molecule remain parallel, traveling in the same direction at a constant speed without coming into contact. This feature reflects the high degree of stability and consistency in the dynamical behavior of soliton molecules. Furthermore, there are noticeable periodic oscillations in the distance between solitons as the propagation distance increases. The initial stability and integrity of soliton molecule are maintained because, in spite of these oscillations, its general structure mostly stays the same. This distinct dynamical behavior suggests that soliton molecules preserve global stability during propagation while displaying dynamic local changes. These features offer important theoretical and experimental support for researching the propagation.

5. THE LUMP SOLUTIONS OF THE NEW $(3+1)$-DIMENSIONAL COMBINED pKP-BKP EQUATION

By referring to previous works [19–22], and applying the Hirota bilinear formalism, exact rational solutions are derived within nonlinear wave systems through the imposition of a long-wave limit on multisoliton solutions. The special rational function solutions will be the focus of this Section, known as lump solutions. With their energy or amplitude concentrated in a limited area, lump solutions decay in all spatial directions and display a lump-like profile that quickly drops to zero at locations distant from the central region. They differ from traditional soliton solutions, which normally propagate in particular directions without dispersion while retaining

their structural integrity, due to this confined feature. In contrast to solitons, which maintain stability along their propagation axes, lump solutions exhibit stronger spatial confinement because their energy density decays algebraically or exponentially in all spatial dimensions and is dramatically peaked around the core region. Because of these characteristics, lump solutions are especially well-suited for simulating nonlinear fluid dynamics phenomena, such as localized water waves and coherent vortices. These solutions are very useful in oceanographic settings for studying tidal dynamics, wave-turbulence interactions, and mesoscale vortical structures in oceanic circulation systems. Researchers can improve prediction models for wave height, directional spreading, and energy distribution patterns in marine environments by utilizing the mathematical framework of lump solutions. Strong risk reduction techniques against extreme wave events are made possible by these developments, which have a direct impact on crucial applications in offshore structure design, coastal engineering, and marine navigation safety.

When

$$N=2,\quad q_1=\lambda_1 p_1,\quad k_1=\gamma_1 p_1,\quad q_2=\lambda_2 p_2,\quad k_2=\gamma_2 p_2,\quad \psi_1^0=\psi_2^0=i\pi, \tag{44}$$

the f in formula (6) can be rewritten to be a polynomial function if $p_i \to 0\,(i=1,2)$:

$$f=\theta_1\theta_2+\alpha_{12}, \tag{45}$$

where

$$\begin{aligned}\theta_i &= -t\left(a+b\lambda_i+c\mu_i-\frac{\gamma^2\lambda_i^2}{5\alpha}\right)+x+y\lambda_i+z\mu_i \quad (i=1,2),\\ \alpha_{12} &= -\frac{60\alpha\left(\frac{\gamma(\lambda_1+\lambda_2)}{2}+\beta\right)}{\gamma^2\left(\lambda_1-\lambda_2\right)^2}.\end{aligned} \tag{46}$$

Letting $a=b=c=\alpha=\beta=1,\gamma=10,\lambda_1=\lambda_2^*=i,\mu_1=\mu_2=1$, the 1-lump solution of Eq. (5) can be resolved by adding the transformation (6) solved as

$$u_{1-lump}=\frac{2(-44t+2x+2z)}{(-22t+x+z)^2+(y-t)^2+\frac{3}{20}}. \tag{47}$$

The specific behavior of the 1-lump solution u_{1-lump} at different times is shown in Fig. 12.

A localized lump with two peaks, one above and one below the horizontal plane, is created as a result of the concentrated energy distribution, giving the lump peaks and troughs. As a solution to Eq. (5), it is visually apparent that the lump, moving on a continuous background without spreading or collapsing, keeps the control center of waveforms perfectly contoured within a finite space. Nevertheless, the asymptotic background of the lump solution is zero since the lump solution degenerates to 0 as

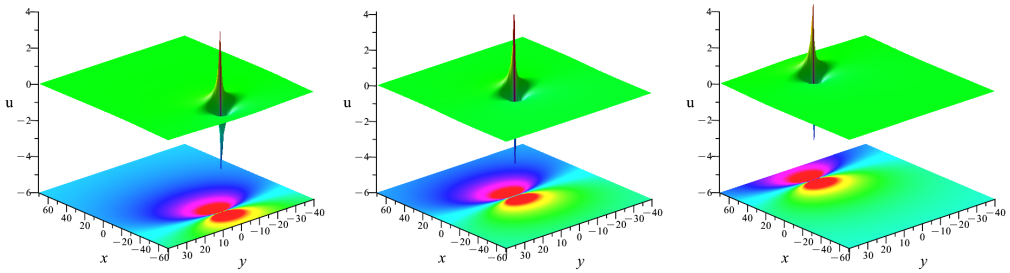

(a) $t=-2$, $z=0$ (b) $t=0$, $z=0$ (c) $t=2$, $z=0$

Fig. 12 – (Color online) The 1-lump solution u_{1-lump} (47) of Eq. (5) on the (x,y) plane at various times.

$x\to\infty$ or $y\to\infty$.

By resetting the parameters in Eq. (24) and Eq. (25) as

$$\begin{aligned} N=4,\quad q_1=\lambda_1 p_1,\quad k_1=\mu_1 p_1,\quad q_2=\lambda_2 p_2,\quad k_2=\mu_2 p_2,\quad q_3=\lambda_3 p_3,\\ k_3=\mu_3 p_3,\quad q_4=\mu_4 p_4,\quad k_4=\mu_4 p_4,\quad \psi_1^0=\psi_2^0=\psi_1^0=\psi_2^0=i\pi, \end{aligned} \tag{48}$$

f in Eq. (24) undergoes a thorough transformation from an exponential function to a completely rational function by letting the limits $p_i\to 0$ $(i=1,2,3,4)$ to get the following formula:

$$\begin{aligned} f=&\theta_1\theta_2\theta_3\theta_4+\alpha_{12}\theta_3\theta_4+\alpha_{13}\theta_2\theta_4+\alpha_{14}\theta_2\theta_3+\alpha_{23}\theta_1\theta_4\\ &+\alpha_{24}\theta_1\theta_3+\alpha_{34}\theta_1\theta_2+\alpha_{12}\alpha_{34}+\alpha_{13}\alpha_{24}+\alpha_{14}\alpha_{23}, \end{aligned} \tag{49}$$

where

$$\begin{aligned} &\theta_i=-t\left(a+b\lambda_i+c\mu_i-\frac{\gamma^2\lambda_i^2}{5\alpha}\right)+x+y\lambda_i+z\mu_i,\\ &\alpha_{ij}=-\frac{60\alpha\left(\frac{\gamma(\lambda_i+\lambda_j)}{2}+\beta\right)}{\gamma^2\left(\lambda_i-\lambda_j\right)^2}\\ &(i<j,i,j=1,2,3,4). \end{aligned} \tag{50}$$

Setting $a=b=c=\alpha=\beta=1,\gamma=5,2\lambda_1=2\lambda_2^*=\lambda_3=\lambda_4^*=2i,\mu_1=\mu_2=\mu_3=\mu_4=1$, and integrating the transformation (6), the 2-lump solution of Eq. (5) is emerged. Besides, the pictorial diagram of the 2-lump solution u_{2-lump} is also presented (see Fig. 13).

The u_{2-lump} undergoes only parallel displacement during asymptotic motion as t evolves, while its permanent lumps pattern remains unchanged. Therefore, the discussion of the lump at $t=0$ is similar. The peaks and valleys of the u_{2-lump}

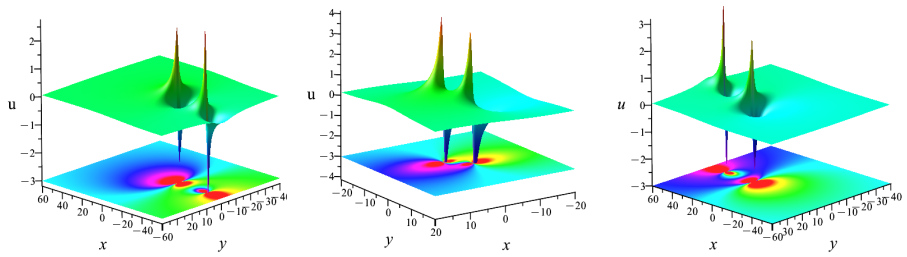

(a) $t=-2,\ z=0$ (b) $t=0,\ z=0$ (c) $t=2,\ z=0$

Fig. 13 – (Color online) The 2-lump solution u_{2-lump} of the Eq. (5) in the $(x,\ y)$ plane.

increase by a factor of two in comparison to the 1-lump solution. Otherwise, the 2-lump solution degenerates to zero and fades away from view as $x\to\infty$ or $y\to\infty$.

6. THE SEMI-RATIONAL SOLUTIONS OF THE NEW $(3+1)$-DIMENSIONAL COMBINED pKP-BKP EQUATION

A wide range of dynamical behaviors, such as elastic collisions, energy exchanges and localization enhancements between lump waves and solitons, are demonstrated by semi-rational solutions, which show the coexistence or interaction between localized waves (like lump solutions) and nonlinear waves (like solitons and breathers). Additionally, the coupling phenomena between ocean surface waves and undersea vortices can be simulated using semi-rational solutions. This has important reference value for forecasting severe wave events (such us freak waves) and for vessel safety design. Consequently, semi-rational solutions advance the classification of exact solutions to mathematical physical equations and uncover new mechanisms of multi-modal wave coupling in nonlinear integrable systems by bridging the gap between pure rational solutions (like lump solutions) and conventional soliton solutions.

The essential factor in the semi-rational solutions of Eq. (5) is the employment of the long-wave limit of the biased exponential function, similar to that in Sec. 5, and the particular restrictions on the parameters in Eq. (24) and in Eq. (25).

Setting the parameters in Eq. (24) and Eq. (25) for $N=3$ as

$$q_1=\lambda_1 p_1,\quad k_1=\gamma_1 p_1,\quad q_2=\lambda_2 p_2,\quad k_2=\gamma_2 p_2,\quad \psi_1^0=\psi_2^0=i\pi, \tag{51}$$

then f in formula (6) can be rewritten as a composite function of exponential and polynomial functions by letting $p_i\to 0\ (i=1,2)$:

$$f=(\theta_1\theta_2+\alpha_{13}\theta_2+\alpha_{23}\theta_1+\alpha_{13}\alpha_{23}+\alpha_{12})e^{\psi_3}+\theta_1\theta_2+\alpha_{12}, \tag{52}$$

where

$$\alpha_{i3}=-\frac{30\alpha p_3^2\left(5\alpha p_3^3+\gamma\lambda_i p_3+2\beta p_3+\gamma q_3\right)}{25\alpha^2 p_3^6+15\left(\frac{\gamma\lambda_i}{3}+\beta\right)\alpha p_3^4+10\alpha\gamma p_3^3 q_3+\gamma^2\lambda_i^2 p_3^2-2\gamma^2\lambda_i p_3 q_3+\gamma^2 q_3^2}\quad(i=1,2), \tag{53}$$

and ψ_3 is the same as in Eq. (25), θ_i $(i=1,2)$, α_{12} are identical to the formula (46). In particular, if the parameters $\lambda_2=\lambda_1^*=i$ and all of the other parameters are actual numbers, for instance, setting $a=b=c=\alpha=\beta=1,\gamma=5,p_3=-q_3=k_3=1,\psi_3^0=0$, then the semi-rational solution of Eq. (5), which contains the 1-kink soliton solution and 1-lump solution, can therefore be written as follows through integrating the transformation (6):

$$u_{lump-1s}=2\frac{(\frac{-852}{229}+\delta_1)e^{\psi}+(\frac{5907}{1145}-\mu_1^*\delta_2-\mu_1\delta_3+\delta_2\delta_3)e^{\psi}+\delta_1}{(\frac{5907}{1145}-\mu_1^*\delta_2-\mu_1\delta_3+\delta_2\delta_3)e^{\psi}+\delta_2\delta_3+\frac{3}{5}}, \tag{54}$$

where

$$\begin{aligned}
&\delta_1=-14t+2x+2z,\\
&\delta_1=(-7+i)t+x-iy+z,\\
&\delta_3=-(7+i)+x+iy+z,\\
&\eta=7t+x-y+z,\\
&\mu_1=\frac{426}{229}+\frac{240}{229}i.
\end{aligned} \tag{55}$$

Because of the elastic nature of their collision, energy will focus at the site of interaction as the amplitude grows. It was clarified the dynamic properties of semi-rational solution of Eq. (5) composed of 1-lump solution and 1-kink soliton (see Fig. 14).

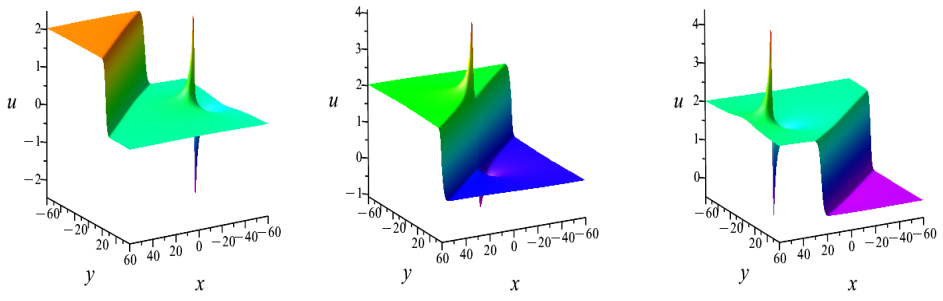

(a) $t=-5,z=0$ (b) $t=0,z=0$ (c) $t=5,z=0$

Fig. 14 – (Color online) The 1-lump solution and 1-kink soliton $u_{lump-1s}$ (54) of Eq. (5) in the (x,y) plane.

When $N=4$, setting the parameters in Eq. (24) and in Eq. (25) as

$$q_1=\lambda_1 p_1,\quad k_1=\gamma_1 p_1,\quad q_2=\lambda_2 p_2,\quad k_2=\gamma_2 p_2,\quad \psi_1^0=\psi_2^0=i\pi, \tag{56}$$

then f in formula (6) can be rewritten in the following form by letting $p_i\to 0\,(i=1,2)$

$$\begin{aligned} f=&(\theta_1\theta_2+\alpha_{13}\theta_2+\alpha_{23}\theta_1+\alpha_{13}\alpha_{23}+\alpha_{12})e^{\psi_3}\\ &+(\theta_1\theta_2+\alpha_{14}\theta_2+\alpha_{24}\theta_1+\alpha_{14}\alpha_{24}+\alpha_{12})e^{\psi_4}\\ &+(\theta_1\theta_2+\alpha_{13}\theta_2+\alpha_{14}\theta_2+\alpha_{23}\theta_1+\alpha_{24}\theta_1\\ &+\alpha_{13}\alpha_{23}+\alpha_{13}\alpha_{24}+\alpha_{14}\alpha_{23}+\alpha_{14}\alpha_{24}\\ &+\alpha_{12})e^{\psi_3+\psi_4+A_{34}}+\theta_1\theta_2+\alpha_{12}, \end{aligned} \tag{57}$$

where

$$\alpha_{i4}=-\frac{30\alpha p_4^2\left(5\alpha p_4^3+\gamma\lambda_i p_4+2\beta p_4+\gamma q_4\right)}{25\alpha^2 p_4^6+15\left(\frac{\gamma\lambda_i}{3}+\beta\right)\alpha p_4^4+10\alpha\gamma p_4^3 q_4+\gamma^2\lambda_i^2 p_4^2-2\gamma^2\lambda_i p_4 q_4+\gamma^2 q_4^2}\quad (i=1,2), \tag{58}$$

and $\alpha_{i3}\ (i=1,2)$ are identical to the formula (53) , $\psi_3,\psi_4,e^{A_{34}}$ are equivalent in Eq. (25), $\theta_i\ (i=1,2),\alpha_{12}$ are equivalent in Eq. (46). Here, if setting the parameters $a=b=c=\alpha=-\beta=1,\gamma=10,\lambda_1=\lambda_2^*=i,-\mu_1=-\mu_2=-2p_3=-2p_4=q_3=-2q_4=2k_3=2k_4=2,\psi_3^0=\psi_4^0=0$, and then intergrating Eq. (24), the semi-rational solution of Eq. (5), which consists of the 2-kink soliton solution and 1-lump solution, can subsequently be generated (see Fig. 15(a)). Nevertheless, a type of semi-rational solutions of Eq. (5) can be formed when the parameters $\lambda_1=\lambda_2^*=i,2\mu_1=\mu_2=2$, and the other two sets of parameters are limited to be complex conjugate. If we take the remaining parameters $a=b=c=\alpha=-\beta=1,\gamma=3,p_3=p_4^*=k_3=k_4^*=2i,q_3=q_4^*=2-i,\psi_3^0=\psi_4^0=2\pi$, the semirational solution, which consists of the 1-breather solution and the 1-lump solution, can be derived (see Fig. 15(b)). The 1-lump and 1-breather solutions to the $(3+1)$-dimensional combined pKP-BKP equation with choosing parameters ($a=b=c=\alpha=\beta=1,\gamma=10,\lambda_1=\lambda_2^*=i,\mu_1=\mu_2=1,p_3=p_4^*=k_3=k_4^*=1-2i,q_3=q_4^*=1-i,\psi_3^0=\psi_4^0=2\pi$) are displayed in Fig. 15(c). In the case of these lump-breather and lump-soliton semirational solutions,when $\psi_i^0\to 0\,(i=3,4)$, the 2-kink soliton will come into collision with the lump of Eq. (5) (see Fig. 15(a)). When $|\psi_i^0|\gg 0\,(i=3,4)$, the lump will undergo a complete separation from the breather solutions of Eq. (5). The breather solutions' amplitude and periodicity will not change (see Figs. 15(b) and (c)).

7. CONCLUSIONS

This paper provides a systematic investigation of several exact solutions of the the new $(3+1)$-dimensional combined pKP-BKP equation and their dynamic

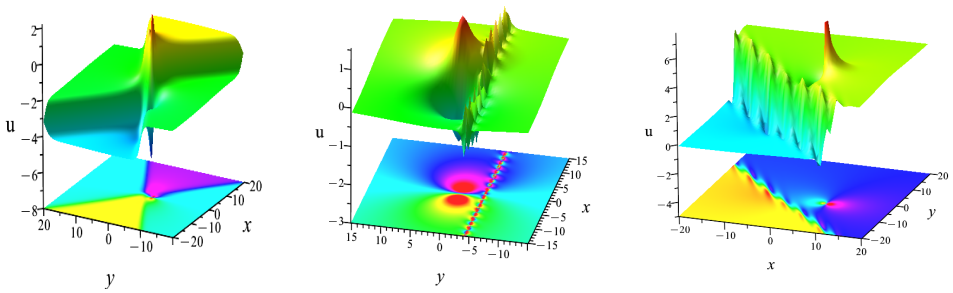

(a) $t = 0, z = 0$ (b) $t = 0, z = 0$ (c) $t = 0, z = 0$

Fig. 15 – (Color online) (a) The 1-lump solution and 2-kink soliton $u_{lump-2s}$ of Eq. (5) in the (x, y) plane at $z = 0$, $t = 0$, (b), (c) The 1-lump solution and 1-breather solution $u_{lump-1b}$ of Eq. (5) in the (x, y) plane at $z = 0$, $t = 0$.

behaviors. Based on standard perturbation method and the Hirota bilinear method, explicit N-soliton solutions of Eq. (5) are derived. The presence of kink properties in the multi-soliton solutions of the Eq. (5) can be attributed to the condition $p_i \neq 0$ $(i = 1, 2 \ldots, N)$ (see Figs. 1 and 2). By introducing restrictions to the parameters of the N-soliton solutions, the high-order breathers with periodic oscillation and localization on the (x, y) plane of Eq. (5) are obtained (see Figs. 3–5). The dynamical characteristics among the various solution types in Eq. (5) are enhanced by mixed solutions made up of breathers and kink solitons (see Fig. 6). The formation of soliton molecular structures is achieved through the derivation of resonance criteria across (x, y), (y, z), and (x, z) planes, utilizing N-soliton configurations (see Figs. 7–11). Additionally, several new hybrid interaction solutions are created, one of which is the dynamic interplay among solitons and the soliton molecule (see Figs. 10 and 11).

Furthermore, the long-wave limit of the soliton solution from Eq. (5) is utilized to form the lump solution (see Figs. 12 and 13). The lump solution is localized only in space. The dynamical behavior of Eq. (5) for $N > 2$ can be better described by using a semi-rational construct comprising lump solution, kink solitons, and breather solutions (see Figs. 14 and 15). Some special constraints on the parameters exert a considerable influence on the diversity and dynamical behavior of these solutions. The constructed solutions in this paper's analysis exhibit dynamical behaviors that reflect the astonishing orderliness resulting from nonlinear interactions. The paper enhances the theory of nonlinear dynamical systems, advances the study of $(3+1)$-dimensional nonlinear evolution equations and aids in explaining certain nonlinear physical phenomena found in nature.

Acknowledgements. This work is supported by the Zhejiang Provincial Natural Science Foundation of China under Grant No. LY24A010002, the Natural Science Foundation of Ningbo under Grant No. 2023J126, Natural Science Research Project of Universities in Anhui Province under Grant No. 2024AH040202.

REFERENCES

1. C. Gu, B. Guo, Y. Li *et al.*, *Soliton Theory and Its Applications*, Springer, Berlin (1995).
2. N.J. Zabusky, M.D. Kruskal, *Interaction of "solitons" in a collisionless plasma and the recurrence of initial states*, Phys. Rev. Lett. **15**, 240–243 (1965).
3. R. Hirota, *Exact N-soliton solutions of the wave equation of long waves in shallow waters and in nonlinear lattices*, J. Math. Phys. **14**, 810–814 (1973).
4. M.J. Ablowitz, J. Villarroel, *Solutions to the time dependent Schrödinger and the Kadomtsev-Petviashvili equations*, Phys. Rev. Lett. **78**, 570 (1997).
5. C. Wang, L. Wang, X. Li *et al.*, *Few-layer bismuthene for femtosecond soliton molecules generation in Er-doped fiber laser*, Nanotechnology **30**, 025204 (2018).
6. C.S. Gardner, J.M. Greene, M.D. Kruskal, R.M. Miura, *Method for solving the Korteweg-de Vries equation*, Phys. Rev. Lett. **19**, 1095 (1967).
7. V.E. Zakharov, A.B. Shabat, *A scheme for integrating the nonlinear equations of mathematical physics by the method of the inverse scattering problem*, I. Funktsional. Anal. i Prilozhen. **8**, 43–53 (1974).
8. M.J. Ablowitz, P.A. Clarkson, *Solitons, nonlinear evolution equations and inverse scattering* (Cambridge University Press, Cambridge, 1991).
9. V.B. Matveev, M.A. Salle, *Darboux transformations and solitons* (Springer, Berlin, 1991).
10. C. Gu, H. Hu, Z. Zhou, *Darboux transformations in integrable systems: theory and their applications to geometry* (Springer, Berlin, 2005).
11. X. Geng, Y. Lv, *Darboux transformation for an integrable generalization of the nonlinear Schrödinger equation*, Nonlinear Dyn. **69**, 1621–1630 (2012).
12. W.X. Ma, A. Abdeljabbar, *A bilinear Bäcklund transformation of a (3+ 1)-dimensional generalized KP equation*, Appl. Math. Lett. **25**, 1500-1504 (2012).
13. J. Hietarinta, N. Joshi, F.W. Nijhoff, *Discrete systems and integrability* (Cambridge University Press, Cambridge, 2016).
14. Z.Z. Lan, Y.T. Gao, J.W. Yang *et al.*, *Solitons, Bäcklund transformation and Lax pair for a (2+1)-dimensional Broer-Kaup-Kupershmidt system in the shallow water of uniform depth*, Commun. Nonlinear Sci. Numer. Simul. **44**, 360-372 (2017).
15. R. Hirota, *The direct method in soliton theory* (Cambridge University Press, Cambridge, 2004).
16. R. Hirota, *Exact solution of the Korteweg-de Vries equation for multiple collisions of solitons*, Phys. Rev. Lett. **27**, 1192 (1971).
17. J. Hietarinta, *Introduction to the Hirota Bilinear Method*, Integrability of Nonlinear Systems, pp. 95-103 (Springer, Heidelberg, 1997).
18. A.M. Wazwaz, *Multiple-soliton solutions for the KP equation by Hirota's bilinear method and by the tanh-coth method*, Appl. Math. Comput. **190**, 633–640 (2007).
19. M.J. Ablowitz, J. Satsuma, *Solitons and rational solutions of nonlinear evolution equations*, J. Math. Phys. **19**, 2180–2186 (1978).
20. J.G. Rao, K. Porsezian, J.S. He, *Semi-rational solutions of the third-type Davey-Stewartson equation*, Chaos **27**, 083115 (2017).

21. J.G. Rao, Y. Cheng, J.S. He, *Rational and semirational solutions of the nonlocal Davey-Stewartson equations*, Stud. Appl. Math. **139**, 568–598 (2017).
22. Y.L. Cao, J.S. He, D. Mihalache, *Families of exact solutions of a new extended (2+1)-dimensional Boussinesq equation*, Nonlinear Dyn. **91**, 2593–2605 (2018).
23. B.B. Kadomtsev, V.I. Petviashvili, *On the stability of solitary waves in weakly dispersing media*, Sov. Phys. Dokl. **15**, 539–541 (1970).
24. G. Huang, V.A. Makarov, M.G. Velarde, *Two-dimensional solitons in Bose-Einstein condensates with a disk-shaped trap*, Phys. Rev. A. **67**, 023604 (2003).
25. C.A. Jones, P.H. Roberts, *Motions in a Bose condensate. IV. Axisymmetric solitary waves*, J. Phys. A: Math. Gen. **15**, 2599 (1982).
26. S. Turitsyn, G. Fal'kovich, *Stability of magnetoelastic solitons and self-focusing of sound in antiferromagnets*, Zh. Eksp. Teor. Fiz. **89**, 7 (1985).
27. Z. Dai, J. Liu, Z. Liu, *Exact periodic kink-wave and degenerative soliton solutions for potential Kadomtsev-Petviashvili equation*, Commun. Nonlinear Sci. Numer. Simul. **15**, 2331–2336 (2010).
28. X. Liu, Q. Zhou, A. Biswas *et al.*, *The similarities and differences of different plane solitons controlled by (3+1)-dimensional coupled variable coefficient system*, J. Adv. Res. **24**, 167–173 (2020).
29. S.L. Xu, Q. Zhou, D. Zhao *et al.*, *Spatiotemporal solitons in cold Rydberg atomic gases with Bessel optical lattices*, Appl. Math. Lett. **106**, 106230 (2020).
30. H. Wang, Q. Zhou, W. Liu, *Exact analysis and elastic interaction of multi-soliton for a two-dimensional Gross-Pitaevskii equation in the Bose-Einstein condensation*, J. Adv. Res. **38**, 179–190 (2022).
31. Z.W. Yan, S.Y. Lou, *Special types of solitons and breather molecules for a (2+1)-dimensional fifth-order KdV equation*, Commun. Nonlinear Sci. Numer. Simul. **91**, 105425 (2020).
32. V.I. Kruglov, H. Triki, *Interacting solitons, periodic waves and breather for modified Korteweg-de Vries equation*, Chinese Phys. Lett. **40**, 090503 (2023).
33. S.Y. Zhu, D.X. Kong, S.Y. Lou, *Dark Korteweg-de Vries system and its higher-dimensional deformations*, Chinese Phys. Lett. **40**, 080201 (2023).
34. A.M. Wazwaz, *Abundant solutions of distinct physical structures for three shallow water waves models*, Discontinuity, Nonlinearity, and Complexity **6**, 295–304 (2017).
35. A.M. Wazwaz, *A variety of distinct kinds of multiple soliton solutions for a (3+1)-dimensional nonlinear evolution equation*, Math. Method. Appl. Sci. **36**, 349–357 (2013).
36. W.X. Ma, *N-soliton solution of a combined pKP-BKP equation*, J. Geom. Phys. **165**, 104191 (2021).
37. A.M. Wazwaz, *Breather wave solutions for an integrable (3+1)-dimensional combined pKP-BKP equation*, Chaos, Solitons and Fractals **182**, 114886 (2024).
38. A.M. Wazwaz, *New Painlevé integrable (3+1)-dimensional combined pKP-BKP equation: lump and multiple soliton solutions*, Chinese Phys. Lett. **40**, 120501 (2023).
39. H. Luo, C. Guo, Y. Guo *et al.*, *Breathing wave solutions and Y-type soliton soluions of the new (3+1)-dimensional pKP-BKP equation*, Nonlinear Dyn. **112**, 20129–20139 (2024).
40. Y. Feng, S. Bilige, *Resonant multi-soliton, M-breather, M-lump and hybrid solutions of a combined pKP-BKP equation*, J. Geom. Phys. **169**, 104322 (2021).
41. K.U. Tariq, A.M. Wazwaz, R.N. Tufail, *Lump, periodic and travelling wave solutions to the (2 + 1)-dimensional pKP-BKP model*, Eur. Phys. J. Plus **137**, 1100 (2022).
42. M. Stratmann, T. Pagel, F. Mitschke, *Experimental observation of temporal soliton molecules*, Phys. Rev. Lett. **95**, 143902 (2005).
43. G. Herink, F. Kurtz, B. Jalali *et al.*, *Real-time spectral interferometry probes the internal dynamics of femtosecond soliton molecules*, Science **356**, 50–54 (2017).

44. X. Liu, X. Yao, Y. Cui, *Real-time observation of the buildup of soliton molecules*, Phys. Rev. Lett. **121**, 023905 (2018).

45. L.C. Crasovan, Y.V. Kartashov, D. Mihalache *et al.*, *Soliton "molecules": robust clusters of spatiotemporal optical solitons*, Phys. Rev. E **67**, 046610 (2003).

46. C.Y. Yin, N.G. Berloff, V.M. Pérez-García *et al.*, *Coherent atomic soliton molecules for matter-wave switching*, Phys. Rev. A **83**, 051605 (2011).

47. B.Q. Li, Y.L. Ma, *Hybrid soliton and breather waves, solution molecules and breather molecules of a (3+1)-dimensional Geng equation in shallow water waves*, Phys. Lett. A **463**, 128672 (2023).

48. Z.W. Yan, S.Y. Lou, *Soliton molecules in Sharma-Tasso-Olver-Burgers equation*, Appl. Math. Lett. **104**, 106271 (2020).